

# Interferometric noise suppression in fiber Bragg grating sensors by using wavelet filter

C.C. CHAN, N. NI\*, J. SUN, Y.C. CHU<sup>a</sup>, Y. TANG<sup>a</sup>, C. L. POH

*NI.3-B3-14, Division of Bioengineering, School of Chemical and Biomedical Engineering, Nanyang Technological University, 70 Nanyang Avenue, Singapore 637457*

*<sup>a</sup>School of Electrical and Electronic Engineering, Nanyang Technological University, Singapore, 639798*

Wavelet digital filter is designed and demonstrated to reduce the wavelength detection error caused by interferometric noise in a fiber Bragg grating (FBG) strain sensor. Simulation and experimental results show that the wavelet filtering technique is a promising approach to enhance the detection accuracy of the FBG strain sensor.

(Received May 31, 2010; accepted June 16, 2010)

*Keywords:* Fiber Bragg grating, wavelet filter, Strain sensor, Interferometric noise

## 1. Introduction

Over the past decade, strain sensing systems have become increasingly important in wide applications including geography, aerospace, structural monitoring, chemical and biomedical sectors. Optical fiber strain sensors outperform mechanical and other sensing counterparts with their specific features depending on the fibers themselves such as high sensitivity, low cost, light weight as well as immunity to electromagnetic interference. Fiber Bragg gratings (FBGs), which are formed by coupling of light to the reverse-propagating guided mode, are proposed as simple yet versatile fiber strain sensors.

However, in order to measure strain variation with high accuracy, detection of the small shift in Bragg wavelength is essential. Several schemes have been reported for detecting the Bragg wavelength shift in FBG sensors [1]. Among all the wavelength detection techniques, the most popular method is the peak detection technique, which uses a tunable laser source to scan through the spectrum of light reflected from the FBG and measures the filter wavelength corresponding to the maximum of the system output [2]. The peak detection technique can be applied to interrogate a number of FBG sensors based on wavelength division multiplexing (WDM) principle. However, in FBG sensor systems using a laser source, although the signal power is relatively high comparing with that using broadband light source, interference between signal waves and other residual reflected waves in the system may cause so-called interferometric noise [3]. This sort of noise might be larger than the source and detector noises and would set a limit on the wavelength detection accuracy of the conventional peak detection technique. Investigation on this interferometric noise in a FBG strain sensor was reported in previous papers. Several signal processing methods,

e.g., finite impulse response (FIR) filter [2] and wavelength modulation technique [4], have been proposed to improve the detection accuracy.

The discrete wavelet transform (DWT) to determine the Bragg wavelength of the FBG was first proposed for a multiplexed fiber Fizeau interferometers (FFI) and FBG sensor system in 2006, by Wong et al. [5,6]. After that, a digital wavelet filter was proposed to reduce the white noise in a broadband light source FBG sensing system in our previous work [7]. In this paper, the use of digital wavelet algorithm to remove the interferometric noise in the FBG sensing systems and enhance the FBG strain measurement capability is proposed. The principle and simulation are described in Section 2, followed by the experiments and experimental results, which are given in Section 3.

## 2. Principle and simulation

In the simulation, the reflection spectrum  $R(\lambda)$  of a FBG with a Bragg wavelength  $\lambda_B$  and a spectral full width at half-maximum (FWHM) symbolized as  $\Delta\lambda_B$  is estimated as a Gaussian distribution of [3]

$$R(\lambda) = R_o \exp \left[ -4 \ln 2 \left( \frac{\lambda - \lambda_B}{\Delta\lambda_B} \right)^2 \right] \quad (1)$$

where  $R_o$  is the maximum reflectivity that occurs at the Bragg wavelength. The spectrum of the reflected light at the photodetector could be written as

$$I_s(\lambda) = \frac{I_o}{4} R(\lambda) = \frac{I_o}{4} R_o \exp \left[ -4 \ln 2 \left( \frac{\lambda - \lambda_B}{\Delta\lambda_B} \right)^2 \right] \quad (2)$$

where  $I_o$  is the initial intensity of the light source, and the factor 1/4 is due to the 3dB directional coupler, as shown in Fig. 1, case (a).

When there is a noise in the system, the light intensity at the photodetector will, in addition to the ideal signal  $I_s(\lambda)$ , have a noise term  $I_n(\lambda)$ . Due to the existing noise, the contaminated will becomes

$$x(\lambda) = I_s(\lambda) + I_n(\lambda) \quad (3)$$

The noise in the system has various origins, but here a particular type of noise, the interferometric noise is considered. This type of noise is caused by the interference between the signal reflected from the FBG and the residual reflected wave from a reflection point as shown in Fig. 1. Assume the linewidth of the source is very narrow (coherence length is very long), the residual reflected wave from the reflection point will interfere with the signal wave from the FBG and produce an unwanted interferometric signal or called interferometric noise (as shown in case (b), Fig. 1). The interferometric noise for this particular case could be written as [2]

$$I_n(\lambda) = \frac{I_o}{2} \sqrt{\alpha^2 R(\lambda)} (1 - R(\lambda)) \cos\left(\frac{2\pi}{\lambda} n\Delta L + \phi\right) \quad (4)$$

where  $\alpha^2$  is the intensity reflectivity of the reflection point,  $n\Delta L$  is the optical path difference between the signal wave and the reflected wave from the reflection point, and  $\phi$  is a random phase factor caused by environmental disturbance. From the equation, the varies of the noise can be subject to the changes of intensity reflectivity  $\alpha^2$ , the optical path difference  $n\Delta L$  and the phase factor  $\phi$ .

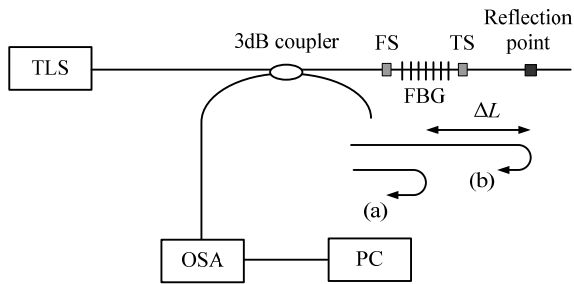


Fig. 1. The setup of the experiment. TLS: tunable laser source; OSA: optical spectrum analyzer; FS: fixed stage; TS: translation stage; PC: personal computer; FBG: fiber Bragg grating.

Wavelet transforms are found increasingly in speech and image processing applications. Their popularity lies in their non-block-based signal decomposition properties which can be tailored for any application [8]. An important application is that wavelet could be functioned as a “filter” or known as wavelet denoising to separate the ideal signal from the contaminated signal [9]. A denoising process starts with the decomposition by the use of multi-resolution analysis (MRA) [10]. In the MRA, the

contaminated signal breaks into shifts and translates of a pair of basis functions, and could be represented as

$$x(\lambda) = \sum_m c_N(m) \phi_{N,m}(\lambda) + \sum_m \sum_{j=N}^{\infty} d_j(m) \psi_{j,m}(\lambda) \quad (5)$$

where  $j, m \in \mathbf{Z}$ , and the integer  $N$  sets the decomposition level,  $\phi_{j,m}(\lambda)$  and  $\psi_{j,m}(\lambda)$  are scaling function and wavelet function respectively, and

$$\begin{aligned} \phi_{j,m}(\lambda) &= 2^{j/2} \phi(2^j t - m) \\ \psi_{j,m}(\lambda) &= 2^{j/2} \psi(2^j t - m) \end{aligned} \quad (6)$$

The DWT coefficients  $c_j$  and  $d_j$  can be computed by a multistage two-channel quadrature filter bank as illustrated as Fig. 2. Each filter bank is formed by the scaling function that acts as a low-pass filter and the wavelet function that acts as a high-pass filter. By decompositions in cascade, the DWT coefficients of the interested level  $N$  are computed, thus the signal can be expressed as

$$x(\lambda) = A_N + \sum_j D_j \quad (7)$$

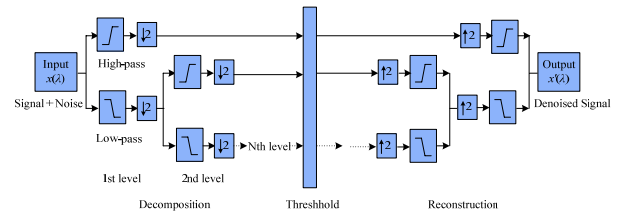


Fig. 2. Block diagram for the DWT-based denoising scheme.

The interferometric noise, in the form of Eq. (2), manifests itself as fine-gained structure of the signal. Therefore, after the decomposition, a threshold operation is applied. If the DWT coefficients are below the threshold, those components  $\sum_j D_j$  will be recognized as noises and removed. Then the reconstruction is performed by inverse discrete wavelet transform (IDWT), the denoising process is fulfilled and  $A_N$  will be the desired ideal signal.

Compared with the commonly used Fourier transform (FT), in which signals are represented as a sum of sinusoids, the highlights of the wavelets are: they could be localized in both time and frequency whereas the FT is only localized in frequency. Moreover, based on multi-resolution analysis, the wavelet processing provides better frequency and time resolution as signals are processed and analyzed at various scale [8].

A key question in the implementation of wavelet transforms is the choice of scaling functions, wavelet functions and the number of signal decomposition levels

[11]. Biorthogonal wavelet is selected in this paper. Biorthogonal wavelet filters evolve from the idea of having an exact reconstruction scheme in which the synthesis filters are different from the analysis filters. Hence the 'orthonormality' condition is relaxed to 'biorthogonality' and implementation advantages in terms of linear phase filters and integer coefficients are possible [12].

Consider an ideal Gaussian reflection spectrum of an FBG sensor corrupted by additional interferometric noise. The FBG has a Bragg wavelength  $\lambda_B$  of 1550 nm, and a FWHM  $\Delta\lambda_B$  of 0.2 nm. The initial intensity of the laser source  $I_o$  is 4  $\mu$ W and the maximum reflectivity that occurs at the Bragg wavelength is equal to 1. The contaminated signal, which varies with the reflectivity parameter of the interferometric noise  $\alpha$ , phase factor  $\phi$  and free spectral range (FSR) (defined as  $FSR = \lambda_B^2/n\Delta L$ ), is realized by using a computer program.

The biorthogonal wavelet Bior6.8 with a level of 5 is applied because it has short support and its symmetric filter coefficients have dyadic rational values enabling the simple arithmetic computation of inner products. Because noise signal will be affected by reflectivity parameter  $\alpha$ , phase factor  $\phi$  and FSR simultaneously by the definition in Eq. (4), and thus the performance of the filter at different  $\alpha$ ,  $\phi$  and FSR needs to be investigated.

The FBG spectrum with noise is sampled from 1549.5 nm to 1550.5 nm with an increment of 1 pm. Assume the phase factor of the noise  $\phi$  is  $\pi/2$ , the reflectivity parameter of the noise is set from 0.1 to 1. The FSR of the noise varies from 0.1 nm to 1 nm. After noise suppressing, the error, which is defined by the peak position shift between the filtered signal and the ideal signal is computed to test the effectivity of the designed filter. The relationship of the error after filtering, the FSR and the reflectivity parameter of the noise is shown in Fig. 3(a). It can be seen that, no matter how much the reflectivity parameter and FSR are, the measurement errors after the wavelet filter keep below 15 pm. When the reflectivity parameter of the interferometric noise is small enough, with the value of 0.1, the error is independently to the FSR of the noise, and the value of the error is quite close to 0, even could be neglected. The maximum error is positioned at the area when FSR is 0.1 nm, i.e.  $n\Delta L=2.45$  cm, while the reflectivity parameter is between 0.6 and 1, with a maximum value of 18.5 pm.

The filtered result is compared with that of a low bandpass finite impulse response (FIR) filter [4]. A Kaiser filter is selected with a filter length of 502 and a cutoff frequency of 0.01 [4]. The filtered result is shown in Fig. 3(b). At FSR of 0.1 nm, the filter performs well and the error after the filter is kept below 10 pm. However, at larger FSRs, the error grows dramatically and the maximum error could reach 74 pm at FSR of 0.5 nm and the reflectivity parameter of 1. At the same FSR, the reflectivity parameter of the noise affects the error after the filter greatly. Normally speaking, the contaminations after the FIR filter become severely with the growth of the noise reflectivity parameter.

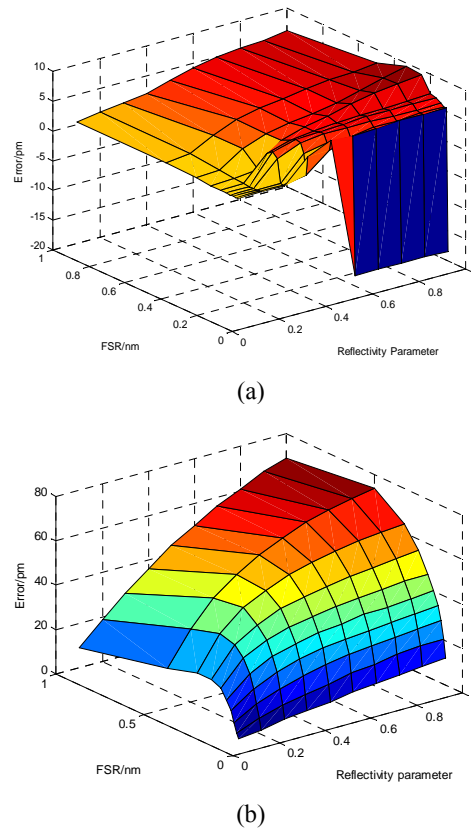
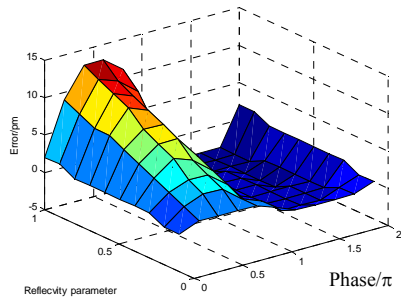


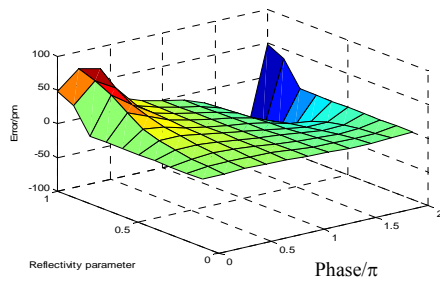
Fig. 3(a). Measurement errors after wavelet filtering at different FSRs and reflectivity parameters of the noise. (b). Measurement errors after FIR filtering at different FSRs and reflectivity parameters of the noise.

With a fix phase factor of  $\pi/2$ , the performance of wavelet filter highlights over FIR filter as a whole. It possesses much smaller minimum and maximum errors than FIR filter, and excluding at FSR of 0.1 nm, all the errors after filter at different FSRs and reflectivity parameters of noise keeps below 10 pm, which means the type of filter is less selective to the FSR and reflectivity parameter of the interferometric noise. In practice, with unknown noise parameters, the wavelet filter is more promising to present better filtered results than those of FIR filter, which is a desirable property for the wavelet filter.

Similar investigations are simulated when the FSR and the reflectivity parameter of the noise are fixed. The filtered results by wavelet filter and FIR filter are shown in Fig. 4 and Fig. 5 respectively. Fig. 4(a) shows the relationship of the reflectivity parameter of the noise, the phase factor and the error after FIR filtering, with a fixed FSR of 1 nm. It is clear that, at the range of the phase factor from  $\pi$  to  $2\pi$ , the error brought by interferometric noise is compensated by wavelet filter below to 3 pm; On the other hand, when the phase factor is between 0 and  $0.8\pi$ , the error after the filter enhances with the reflectivity parameter of noise. The largest error is obtained at  $\alpha=1$ ,  $\phi=0.4\pi$ , with a value of 13 pm.

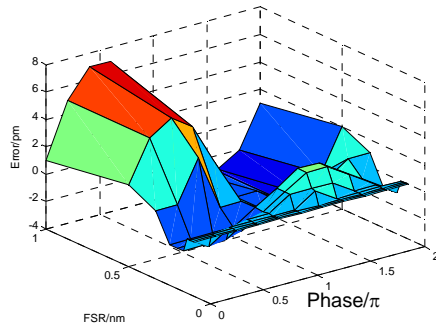


(a)

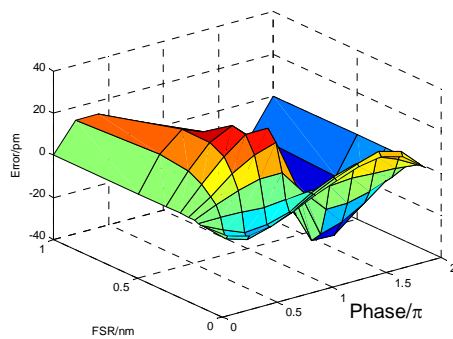


(b)

Fig. 4(a). Measurement errors after wavelet filtering at different reflectivity parameters and phase factors of the noise. (b). Measurement errors after FIR filtering at different reflectivity parameters and phase factors of the noise.



(a)



(b)

Fig. 5(a). Measurement errors by wavelet filtering at different FSRs and phases of the noise. (b). Measurement errors by FIR filtering at different FSRs and phases of the noise.

FIR is applied to the simulation signal too, and the filtered result is as shown in Fig. 4(b). Compared with wavelet filter, the filtered error only could be kept below 3 pm at the reflectivity parameter of the noise of 0.1. At the same phase value, the error also increases with the enhancement of reflectivity parameter of the noise. The worst case occurs at  $\alpha=1$ ,  $\phi=1.8\pi$ , and the error could reach to as large as 76 pm.

When the reflectivity parameter of the noise is fixed to 0.5, the filtered errors by the wavelet filter and FIR filter are shown in Fig. 5(a) and (b) respectively. For the wavelet filter, the error after filtering is able to be kept below 2 pm when the FSR of the noise is at the range between 0.1 nm and 0.25 nm. The error is maximized as 7 pm when FSR is equal to 1 nm and the phase factor is equal to  $0.4\pi$ . The error after the FIR filter, however, has a maximum error of 31 pm, at FSR=0.25 nm,  $\phi=1.4\pi$ , 4 times larger than that after the wavelet filter.

### 3. Experiments and experimental results

Experiment was conducted using the setup shown in Fig. 1. Light from the LED with the power about  $30 \mu\text{W}$  passed through a 50/50 coupler and then was fed into a FBG. The reflected light from the FBG was guided back through the same coupler to an optical spectrum analyzer (OSA) that analyzed the reflected signal. The wavelength range of the OSA was set from 1549.5 to 1550.5 nm and sampled by 1000 points, corresponding to a step size of 1 pm. The FBG was held by a fixed stage (FS) and a translation stage (TS). Strain could be applied on the FBG by manually tuning the TS. The 'ideal' reflection spectrum was measured by breaking the fiber end manually, while the noisy reflection spectrum was measured by cleaving the fiber end by a cleaver, which would induce a reflection point and interferometric noise forms. The measurement was repeated for 10 times within 3mins. Within this time period, the Bragg wavelengths of the sensing FBGs could be regarded to be constant. The Bragg wavelength was only measured once for each strain step and the strain step used was  $25 \mu\epsilon$ . Both reflection spectra were changed to arbitrary unit for the convenience of analysis.

The measurement errors varying with independent times and steps are investigated as in Fig. 6(a). Both of the number of steps and times are 10. In this  $10 \times 10$  measurements, the minimum measurement error of 0.2 pm was achieved. The corresponding original, contaminated and filtered spectra are shown in Fig. 6(b). It is clearly shown that the curve shape of the filtered signal is much closer to the original signal than the contaminated signal, which proves the effectivity of the designed filter. The maximum measurement error, from Fig. 6(a), was 6.5 pm. The corresponding filtered spectrum shown in Fig. 6(c) also demonstrates a more similar curve-shape to the original than the contaminated signal. But the detected wavelength had an error and this error was due to the high contamination of the noise, and thus the filter couldn't recognize the peak position correctly from the contaminated signal at this condition.

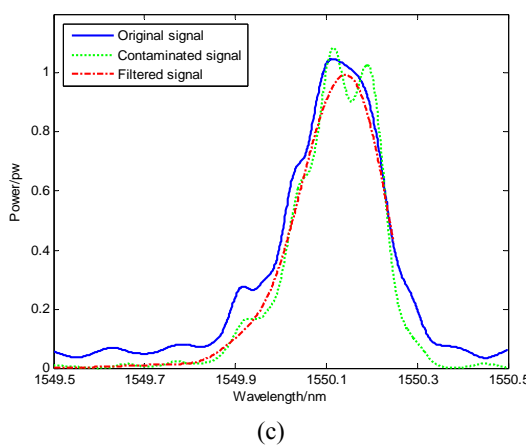
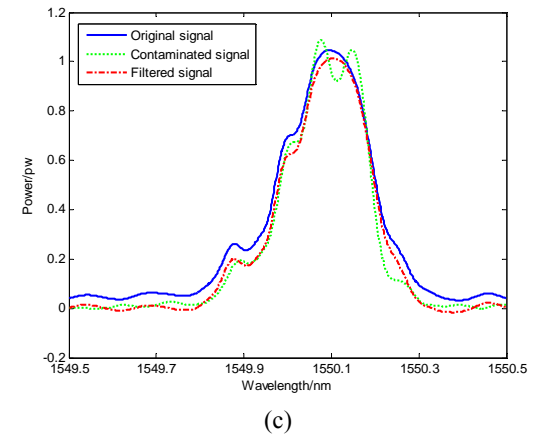
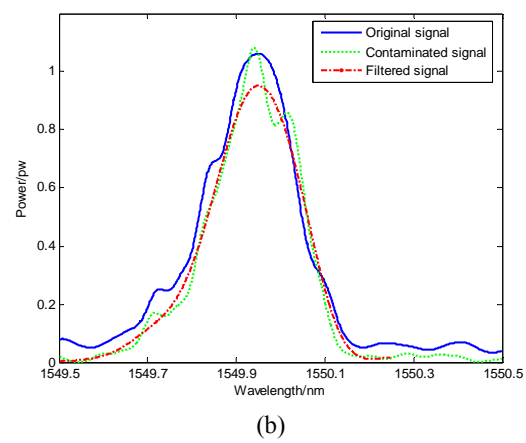
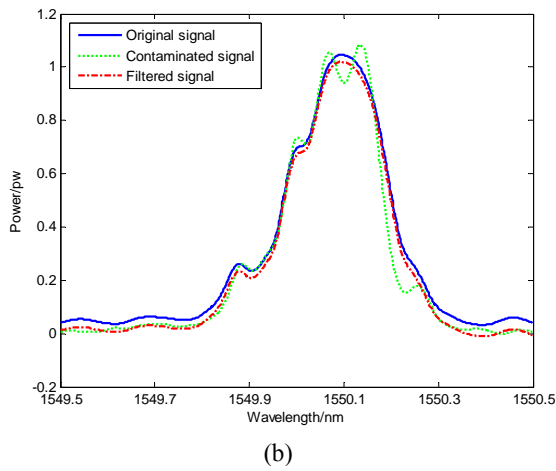
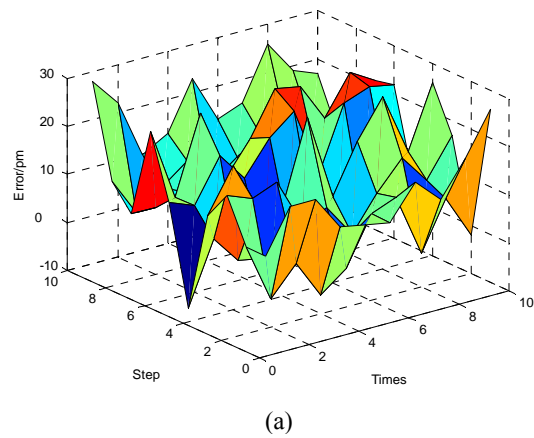
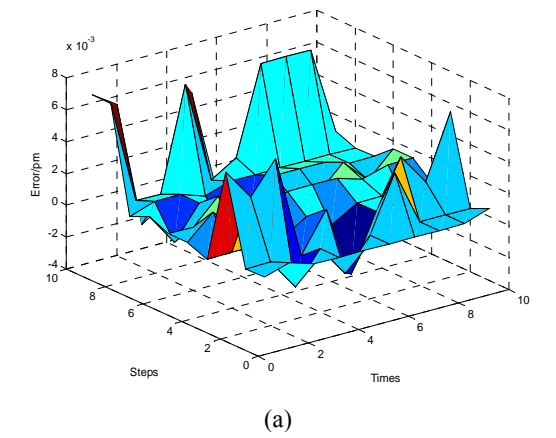


Fig. 6(a). Measurement error by wavelet filtering with step and times.(b). Original, contaminated and wavelet filtered spectra at the minimum error (c). Original, contaminated and wavelet filtered spectra at the maximum error.

Fig. 7(a). Measurement error by FIR filtering with step and times. (b). Original, contaminated and FIR filtered spectra at the minimum error. (c). Original, contaminated and FIR filtered spectra at the maximum error.

Again, the experimental signal was filtered by the aforementioned FIR filter. The filtered measurement errors with the steps and times are as illustrated in Fig. 7(a). It is found that the minimum measurement error of 1 pm and the maximum measurement error of 28 pm are obtained respectively. Compared with those by wavelet filter, the filtered signals not only had larger errors, but also the filtered signals were not intact due to the price of the FIR filter functions. Furthermore, the comparison was also made between the root-mean-square (RMS) measurement errors after filtering by the designed wavelet filter and the FIR filter. The RMS measurement error after the wavelet filter was 4 pm, while the RMS measurement error after the FIR filter was as large as 30 pm. Therefore, by the comparison the wavelet filter is a more promising technique to remove the interferometric noise and to enhance the measurement accuracy in the FBG sensing system.

#### 4. Conclusion

A wavelet filter is designed to reduce the interferometric noise in a FBG sensing network for improving the measurement accuracy. By the theoretical analysis, the interferometric noise parameters, i.e. the reflectivity parameter, the FSR and the phase factor all will influence the measurement performances of the FBG strain sensor. A wavelet filter is designed to reduce the interferometric noise of the sensing system. The specifications of the filter are selected according to the properties of interferometric noise. By simulations, the effects of the reflectivity parameter, the FSR and the phase factor of the noise to the filtered error are investigated. After that, the performance of the wavelet filter is evaluated in both simulation and experiment. The superiority of the wavelet filter is demonstrated by the comparison of a FIR filter. The simulation and experimental results show that the minimum filtered errors by using the wavelet filter are smaller than those by using FIR filter. And filtered errors are definitely less

independent to the noise factors in the use of wavelet filter. Therefore, with proper wavelet function and filter level, the noise of the highly contaminated spectral signal could be successfully suppressed and a minimum error of 0.2 pm is achieved after the well designed wavelet filter.

#### References

- [1] M. G. Xu, H. Geiger, J. P. Dakin, *IEEE/OSA Journal of Lightwave Technology* **14**, 391 (1996).
- [2] C. C. Chan, W. Jin, M. S. Demokan, *Optics & Laser Technology* **31**, 299 (1999).
- [3] W. Jin, *Applied Optics*, **37**(13), 2517 (1998).
- [4] C. C. Chan, J. M. Gong, W. Jin, M. S. Demokan, *Optics Communications* **17**, 3203 (2000).
- [5] A. C. L. Wong, P. A. Childs, G. D. Peng, *Optics Letters*, **31**, 23 (2006).
- [6] A. C. L. Wong, P. A. Childs, G. D. Peng, *Measurement Science & Technology*, **17**, 384 (2006).
- [7] C. C. Chan, N. Ni, J. Sun, *J. Optoelectron. Adv. Mater.* **9**, 2376 (2007).
- [8] G. Strang, T. Nguyen, *Wavelets and Filter Banks*, Wellesley-Cambridge Press (1997).
- [9] M. P. Wachowiak, G. S. Rash, P. M. Quesada, A. H. Desoky, *IEEE Transaction on biomedical engineering* **47**, 360 (2000).
- [10] A. C. L. Wong, P. A. Childs, Gang-Ding Peng, Simultaneous demodulation technique for a multiplexed fiber Fizeau interferometer and fiber Bragg grating sensor system, Vol. 31, No. 1, *Optics Letters*, 2006.
- [11] J. E. Odegard, C. S. Burrus, *IEEE Digital Signal Processing Workshop Proceeding*, 73–76 (1996).
- [12] S. Masud, J. V. McCanny, *IEE Proceeding-Circuits, Devices and Systems* **147**, 293 (2000).

---

\*Corresponding author: nina@pmail.ntu.edu.sg